J Incl Phenom Macrocycl Chem (2016) 85:59–68
DOI 10.1007/s10847-016-0605-4

ORIGINAL ARTICLE

Secondary assembly mechanism of cyclodextrin based on $LiNTf_2$@β-CD system

Jianfeng Shi[1] · **Xinghai Shen**[1]

Received: 24 June 2015 / Accepted: 22 March 2016 / Published online: 30 March 2016

Abstract Cyclodextrin-based nanotubes have been widely investigated and their secondary assembly (SA) behavior was found in our previous works. Here we report the self-assembly behavior between lithium bis(trifluoromethylsulfonyl)imide ($LiNTf_2$) and β-cyclodextrin (β-CD). Nanosheet structures with regular shape were obtained in the concentrated $LiNTf_2$@β-CD solution. This phenomenon can be explained in terms of the SA mechanism of CD induced by the inorganic guest $LiNTf_2$. $LiNTf_2$ and β-CD firstly forms nanotubes, and the nanotubes further stack with each other to form nanosheets by SA. We confirm that the hydrogen-bonding interaction contributes a lot to the formation of the nanotubes and their SA, and Li^+ shows a special effect in the SA by inducing hydrogen-bonding network between the adjacent β-CD to regularly pack the nanotubes.

Keywords β-Cyclodextrin · $LiNTf_2$ · Secondary assembly · Nanosheet

Introduction

Formation of cyclodextrin (CD)-based supramolecular self-assemblies has been the topic of current interest. They were widely investigated from the aggregate of native CDs to high-order self-assemblies [1]. CD nanotubes, as an important type of supramolecular self-assembly have intrigued increasing interest in recent years due to their potential for acting as molecular devices as well as functional materials. It was firstly reported by Agbaria and Gill that 2,5-diphenyloxazole (PPO) can form extended nanotubes with γ-CD at relatively high concentrations [2]. Later Li et al. reported the formation of rigid molecular nanotubes of β-CD and γ-CD with the rodlike molecules all-trans-1,6-diphenyl-1,3,5-hexatriene (DPH) [3]. It is noteworthy that the visualized images of nanotubes were obtained with STM for the first time [3]. Pistolis et al. found that DPH could facilitate the formation of nanotubes with β- and γ-CD in the appropriate solvents [4]. The results of their further study on the size effect of the homologues of the α,ω-diphenylpolyenes series, with two, three, and four double bonds, on the formation of nanotubes with γ-CD indicated that the length of guest molecule is a key factor in the course of nanotube formation [5]. Liu et al. focused on the artificial design of CD nanotubes induced by different CD derivatives and metal ions through the metal–ligand coordination [6–8].

The study of CD nanotubes has been paid much attention, and most of the CD nanotubes were found to be induced by organic molecules, which has become a subject of great interest [9–17]. Interestingly, Agbaria and Gill reported that some oxazole molecules including 2-phenyl-5-(4-diphenylyl) 1,3,4-oxadiazole (PBD) could form inclusion complexes with γ-CD at lower concentrations, which could further form extended nanotubes at relatively high concentrations [2, 12]. Visible turbidity occurred after mixing an equimolar solution of γ-CD with PBD, but no detailed characterization was conducted for the precipitates.

In the past several years, our research group aimed to investigate what kinds of organic molecules cause the formation of CD nanotubes, and has found several organic

✉ Xinghai Shen
xshen@pku.edu.cn

[1] Beijing National Laboratory for Molecular Sciences (BNLMS), Fundamental Science on Radiochemistry and Radiation Chemistry Laboratory, College of Chemistry and Molecular Engineering, Peking University, Beijing 100871, People's Republic of China

molecules [18–25]. Moreover, we also found the precipitation in the PBD-β-CD, 2,5-bis(5′-*tert*-butyl-2-benzoxazoyl)thiophene (BBOT)-β-CD, and BBOT-γ-CD solutions [23–25]. Further characterization suggested for the first time that the precipitates originated from the micrometer-sized rodlike structures, which was assembled by thousands of small nanotubes in a stack way layer by layer. We believe that the organic molecules first induce β-CDs to form rigid nanotubes, and with these nanotubes as crystallization centers, other empty β-CDs are packed to channel in the *c* axis direction and hexagonally aligned in the *b* axis direction. More and more β-CDs deposit together and the micrometer-sized rodlike structures finally form [23–25]. The formation of these self-assemblies is mainly driven by intermolecular hydrogen-bonding, and the secondary assembly (SA) mechanism of CD nanotubes was proposed accordingly [23–25]. The measurements of density and fluorescence microscopy confirmed the fact that both empty and occupied CDs coexisted in the SA [23–25].

Later similar SA structures of CD nanotubes have also been reported by some other research groups [26–33]. Jaffer et al. and Sowmiya et al. found that trans-2-[4-(dimethylamino)styryl]benzothiazole (DMASBT) could induce the formation of CD nanotubes and their rodlike SA [26–28], although they suggested that the SA consisted of nanotubes filled with DMASBT only and no empty CD was involved [28]. Recently, they discovered rodlike SA in a hemicyanine dye, 4-[4-(dimethylamino)-styryl]-1-docosylpyridinium bromide (DASPC22) and β-CD system [29]. It was observed that inorganic salts (e.g. $KClO_4$, KI, KCl, KF) reduced the stability of the supramolecular structures at high concentration, because they acted as salting-in agents and reduced the binding strength between the dye and β-CD, giving H-aggregates of the dye [29]. However, the salts at low concentration enhanced the stability of binding between the host and guest molecules by providing anchor sites for intermolecular hydrogen-bonding between neighboring β-CD molecules. This is possibly because of the strong Coulombic interaction between these ions and the chromophore of the dye [29]. These results indicate that inorganic ions may influence the formation of the CD SA.

The discovery of the CD SA together with other CD aggregation behaviors was regarded as one of the great improvements in CD chemistry [34]. They may act as promising candidates for nanoscopic filters, biosensors, catalysts, and photoresponsive materials. However, so far only a few organic compounds have been found to realize the formation of the SA, and a small amount of SA with rodlike morphology can be obtained due to the limited solubility of these organic molecules. It should be reasonable that some molecules with better solubility can induce more CD molecules to form SA with various morphologies.

Park et al. prepared an anisotropic supramolecular hydrogel from γ-CD-azo dye system [35, 36]. They found that the γ-CD–dye solution turned into hydrogel when the concentrations of the two components increased to about 100 mM. The formation of the hydrogel would be influenced by many metal ions [35]. Especially for Li^+, the physical gelation of the 60 mM γ-CD and 60 mM dye solution was induced by adding LiCl [36]. In the model, fibrous nanotubes were firstly formed by head-to-head γ-CDs, which were held together by the dye molecules in the cavities. Then the nanotubes were bound together by hydrogen-bonding interaction [35]. In the Li^+-hydrogel, the nanotubes were further closely packed by Li^+ in tetragonal interstices by hydrogen-bonding between Li^+ and the neighboring γ-CD [36]. In this example, the hydrogel was apparently formed by the SA of the γ-CD-dye nanotubes, and it should be noted that the host and guest molecules in this SA system can reach a relatively high concentration, so the SA occurs in a large scale to form the macroscopic supramolecular hydrogel. Besides, metal ions, especially Li^+, played a special role in this system [35, 36].

Our research group has been investigating the supramolecular interaction pattern between ionic liquids (ILs) and CDs [37–40], and constructed vesicles and supramolecular hydrogel between ILs and CDs [41, 42]. In our previous studies about the interaction between the IL 1-alkyl-3-methylimidazolium-bis(trifluoromethylsulfonyl) imide ($C_n$mimNTf_2) and β-CD, we reported that NTf_2^- could form inclusion complex with β-CD in the diluted aqueous solution [38, 39]. NTf_2^- showed its ability to interact with CD, so in this work we choose the water-soluble $LiNTf_2$ for the investigation of its further self-assembly with β-CD in the concentrated solution. In the Li^+-NTf_2^--β-CD system, it is expected that NTf_2^- is included in the CD cavity and that there are electrostatic, hydrophobic, and hydrogen-bonding interactions, which is favorable for the self-assembly. It is also expected that novel supramolecular phenomena occur between $LiNTf_2$ and β-CD system. Meanwhile, the addition of Li^+ may influence the hydrogen-bonding interaction, which is one of the main driving force for CD-based self-assembly. So, the important role Li^+ plays in the self-assembly should also be investigated.

Experimental section

Materials

β-CD (Beijing Aoboxing, China) was recrystallized twice and dried under vacuum for 24 h. α-CD (≥98 %, ACROS), γ-CD (≥99 %, ACROS), 2,6-dimethyl-β-CD (DM-β-CD,

J&K Chemical Company) were used as received. $LiNTf_2$ (>99 %) was purchased from Lanzhou Institute of Chemical Physics, China. $HNTf_2$ (99 %) was purchased from J&K Chemical Company. $NaNTf_2$ and $KNTf_2$ was obtained by mixing $HNTf_2$ with NaOH and KOH in the aqueous solution. All other chemicals were analytical grade and used without further purification. Ultrapure water was used throughout the experiments.

Method

Sample preparation

The $LiNTf_2$@β-CD aqueous solutions were prepared by weighing desired amount of $LiNTf_2$ and β-CD, and then heated to obtain transparent solutions, which were kept thermostatically at room temperature for at least 24 h. Then the solutions were freeze-dried for structural characterization. Before freeze-drying, the solutions were quickly freezed by liquid nitrogen to maintain their original self-assembly structure [41, 42].

Dynamic light scattering (DLS)

DLS measurements were performed on an ALV/DLS/SLS-5022F photo correlation spectrometer. The wavelength of laser was 632.8 nm and the scattering angle was 90°. The temperature was controlled at 25 °C. The samples were treated by centrifugating at 10,000 rpm for 30 min before the measurement.

Transmission electron microscope (TEM)

One drop of the sample solution was placed onto a formvar-coated copper grid, and a drop of phosphotungstic acid solution (2 wt%) was used as the negative-staining agent to make the TEM images more clear. For the freeze-fracture TEM (FF-TEM), samples were frozen by liquid propane. The fracturing and replication were carried out on a freeze-fracture apparatus (Balzers BAF400, Germany) at −140 °C. Pt/C was deposited at an angle of 45° to shadow the replicas, and C was deposited at an angle of 90° to consolidate the replicas. The samples were examined on an FEI Tecnai G2 T20 electron microscope operating at 200 kV.

Powder X-ray power diffraction (XRD)

XRD patterns were obtained on a D/MAX-PC2500 diffractometer with Cu-K_α radiation ($\lambda = 0.154056$ nm). The supplied voltage and current were set to 40 kV and 100 mA, respectively. Powder samples were mounted on a sample holder and scanned at a speed of 4°/mim.

Electron spray ionization/mass spectrometry (ESI/MS)

The ESI/MS used with electrospray ionization (ESI) was done on a Fourier transform ion cyclotron resonance mass spectrometer, APEX IV(Bruker, USA).

Fourier transform infrared spectra (FTIR)

FTIR spectra of the grinded xerogel were recorded on a NICOLET iN10 MX spectrometer using infrared microspectroscopy method.

Results

DLS measurements

After being kept thermostatically for at least 24 h, the $LiNTf_2$@β-CD solutions were still clear and no precipitation happened, even the concentration reached 70 mM@70 mM. The $LiNTf_2$@β-CD solutions show obvious Tyndall phenomenon, suggesting the existence of self-assembly in the solutions. Figure 1a shows the DLS result of $LiNTf_2$@β-CD (30 mM@30 mM) solution. The hydrodynamic radius (R_h) ranges from 50 to 300 nm, indicating the existence of large self-assembly. The shape of the self-assembly in the solutions is characterized by TEM method below. α-CD, γ-CD, and DM-β-CD are also utilized (Fig. 1b–d) and only the $LiNTf_2$@γ-CD solution shows the signal of large self-assembly. The signals in Fig. 1b and d, whose diameter is about 1–2 nm, probably derive from β-CD or the NTf_2^--β-CD inclusion complex [22, 23, 42]. In addition, $LiNTf_2$ on its own cannot self-assembly so that no self-assembly signal occurs in Fig. 1e.

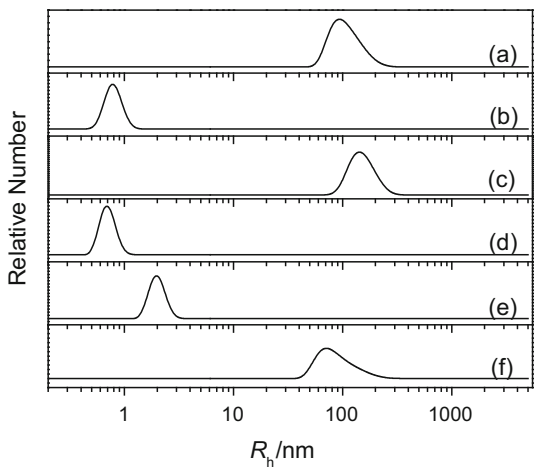

Fig. 1 DLS results of 30 mM@30 mM solutions of $LiNTf_2$ with different CDs: *a* β-CD, *b* α-CD, *c* γ-CD, *d* DM-β-CD; DLS result of *e* 30 mM $LiNTf_2$ solution and *f* 10 mM β-CD solution

In contrast, 10 mM β-CD solution shows a signal (Fig. 1f) whose average size is similar to that of the $LiNTf_2$@β-CD solution. Bonini et al. characterized that β-CD formed globular particles or large planar sheets at different concentrations [43]. We observed large amorphous spherical aggregates in 10 mM β-CD solution [23]. According to the TEM results below, it can be excluded that the self-assembly in the $LiNTf_2$@β-CD solution are the amorphous aggregation of β-CD itself.

We have reported that $LiNTf_2$ mainly forms the 1:1 inclusion complex with β-CD in diluted aqueous solution [39]. In the concentrated solution, the influence of the molar ratio on the self-assembly is firstly investigated by DLS here. Figure 2b–e show that with the addition of $LiNTf_2$ into the 30 mM β-CD solution, there exists self-assembly when the concentration of $LiNTf_2$ is less than 30 mM, but the self-assembly is disassembled into simple inclusion complexes when the concentration of $LiNTf_2$ is above 30 mM. It seems to be a turning point when the molar ratio of $LiNTf_2$ to β-CD is around 1:1. We suggest that the excess β-CD in $LiNTf_2$@β-CD (15 mM@30 mM) solution probably formed the amorphous aggregates itself, while the excess $LiNTf_2$ destroyed the self-assembly.

In Fig. 3 we investigated a series of solutions using $HNTf_2$. $HNTf_2$ is a weak acid (pKa = 1.7) [44] and a large part of $HNTf_2$ remains undissociated in the $HNTf_2$@β-CD solution. Figure 3a shows that the $HNTf_2$@β-CD system cannot self-assemble, and Fig. 3b shows that the addition of H^+ to $LiNTf_2$ destroys the self-assembly, indicating that the dissociated NTf_2^- is necessary for the formation of self-assembly. On the other hand, when some base is added into the $LiNTf_2$@β-CD solutions, the self-assembly is also destroyed (Fig. 3c). It is widely reported that hydrogen-bonding is an important driving force for CD-based self-assembly. The proton dissociation constant of β-CD is 12.20 [45], so the hydroxyl groups on the rim of β-CD turn into O^- in the alkaline environment, which blocks the hydrogen-bonding interaction between adjacent CDs. Besides, according to Fig. 3d and e, there exists self-assembly in all the $LiNTf_2$@β-CD, $NaNTf_2$@β-CD, and $KNTf_2$@β-CD systems, although the size of the self-assembly in the $NaNTf_2$@β-CD and $KNTf_2$@β-CD systems is relatively smaller than that in $LiNTf_2$@β-CD. We believe Li^+ plays a special role in the self-assembly between NTf_2^- and β-CD.

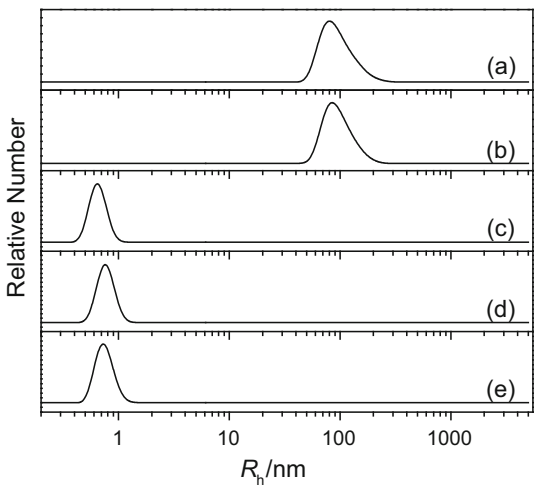

Fig. 2 DLS results of the aqueous solutions of $LiNTf_2$@β-CD at various concentrations: *a* 15 mM@30 mM, *b* 30 mM@30 mM, *c* 40 mM@30 mM, *d* 50 mM@30 mM, *e* 60 mM@30 mM

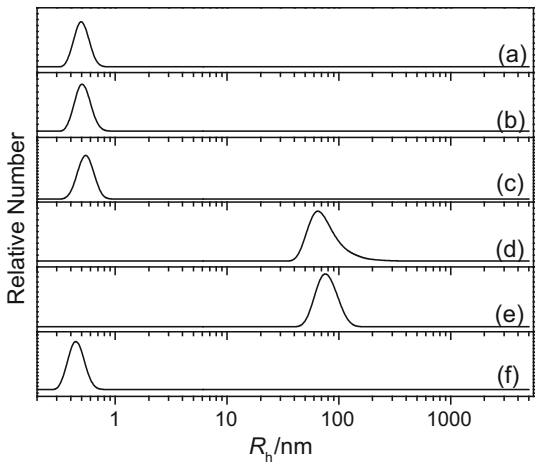

Fig. 3 DLS results of the solutions of *a* $HNTf_2$@β-CD, *b* $LiNTf_2$@β-CD with HCl, *c* $LiNTf_2$@β-CD with LiOH, *d* $NaNTf_2$@β-CD, *e* $KNTf_2$@β-CD, *f* $LiNTf_2$@β-CD with urea. All the components are at the concentration of 30 mM except urea (1 M)

In addition, we investigated the effect of urea on the self-assembly of $LiNTf_2$@β-CD since it is an effective method for characterizing the hydrophobic nature of the interaction between CDs and guest molecules [46, 47]. The self-assembly was destroyed once the urea was add (Fig. 3f).

TEM characterization

The morphologies of the self-assemblies in the $LiNTf_2$@β-CD solutions were examined by negative-staining TEM and FF-TEM. Figure 4a displays nanosheet structures with regular shape, indicating a well-organized arrangement of the component in the self-assembly. The side length of the nanosheets ranges from about 80 to 400 nm, which roughly accords with the size distribution from DLS measurements. As is marked by arrows in Fig. 4a, the thickness of the nanosheets is about 30–40 nm. Figure 4b is the FF-TEM micrograph of the nanosheet in the $LiNTf_2$@β-CD system. The shapes roughly correspond to nanosheet structures after being fractured and replicated. This kind of nanosheet

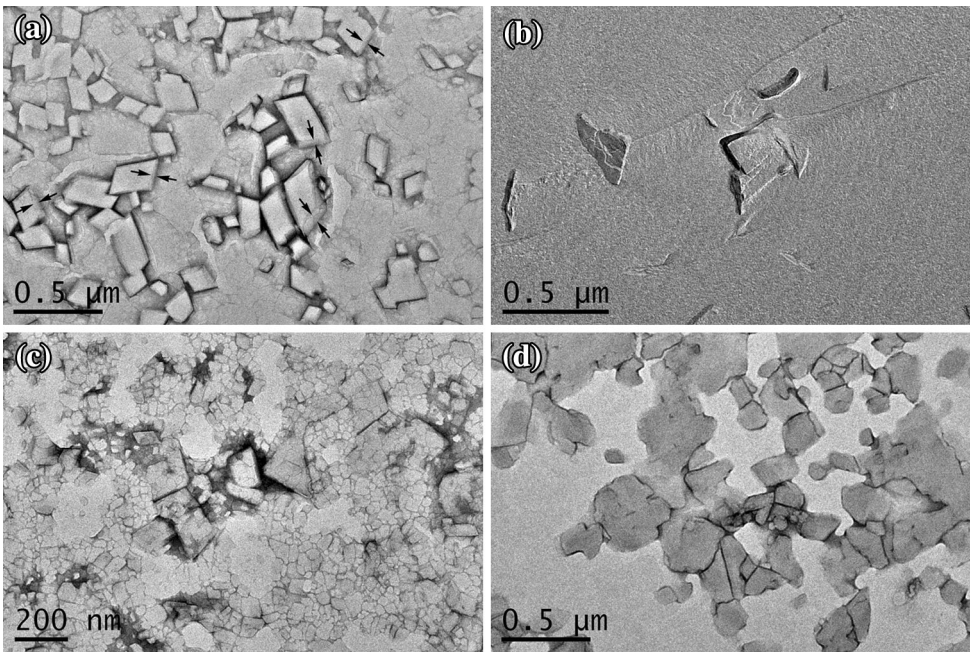

Fig. 4 **a** Negative-staining and **b** FF-TEM micrographs of the $LiNTf_2$@β-CD (30 mM@30 mM) solution. Negative-staining micrographs of **c** $LiNTf_2$@β-CD (15 mM@30 mM) solution and **d** $KNTf_2$@β-CD (30 mM@30 mM)

structure is apparently different from the nanotubes and their SA as reported before [23–29].

Besides, Fig. 4c shows that there exists the mixture of nanosheets and small particles in $LiNTf_2$@β-CD (15 mM@30 mM) solution. We propose that the excessive β-CD does not influence the formation of nanosheets, but forms the amorphous aggregates [23, 43].

Moreover, we observed the morphology of the self-assemblies in the $NaNTf_2$@β-CD and $KNTf_2$@β-CD systems. Figure 4d displays irregular-shaped nanosheets in the $KNTf_2$@β-CD system, and this was also observed in the $NaNTf_2$@β-CD system. These structures are apparently different from those in the $LiNTf_2$@β-CD system and this will be taken into consideration when the self-assembly mechanism is discussed.

XRD patterns

We freeze-dried a series of samples for structural characterization of the self-assembly in the $LiNTf_2$@β-CD aqueous solution. Figure 5d shows the XRD pattern of the freeze-dried product of $LiNTf_2$@β-CD (30 mM@30 mM) solution, which differs from the XRD patterns of the freeze-dried β-CD (Fig. 5f). The structure of β-CD and its complexes are mainly classified into cage-type and channel-type ones. Here the major peaks at $2\theta = 9.5$, 12.6, and 18.2° in Fig. 5f are observed, indicating the cage-type structure of the original β-CD. While the major peaks at $2\theta = 11.5$ and 17.6° in Fig. 5d and e are characteristic of the channel-type of β-CD [48–50]. It can thus be deduced that the β-CD molecules form the channel-type structure in

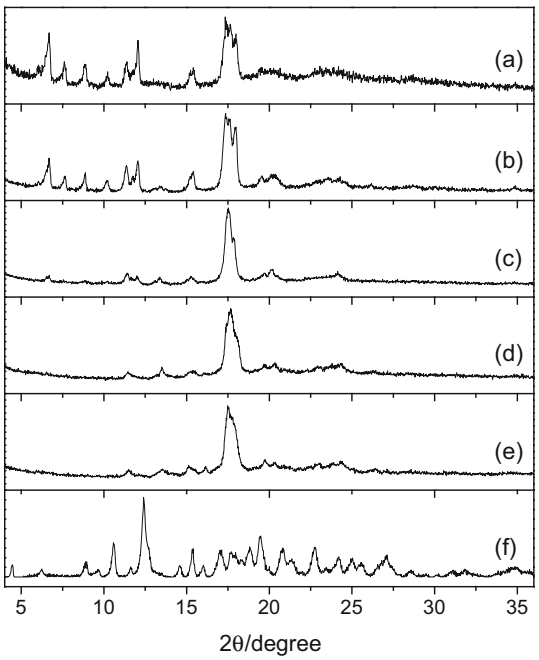

Fig. 5 XRD patterns of freeze-dried products of $LiNTf_2$@β-CD solutions at various concentrations: *a* 10 mM@30 mM, *b* 20 mM@30 mM, *c* 25 mM@30 mM, and *d* 30 mM@30 mM, and that of *e* $KNTf_2$@β-CD (30 mM@30 mM) and *f* β-CD

the self-assembly, probably the nanotube structures. The $LiNTf_2$@β-CD nanotubes should be the structural unit for the formation of the nanosheets. As for $KNTf_2$@β-CD, the channel-type stacking of β-CD also exists although the shape of the nanosheets is not as regular as that of $LiNTf_2$@β-CD system (see Fig. 4).

In addition, comparing Fig. 5a–d, the samples from the non-stoichiometric $LiNTf_2$ and β-CD solution exhibit more signals than that from the 1:1 system. These signals are supposed to originate from the dissociative β-CD aggregate, which also confirms the 1:1 molar ratio of the self-assembly between $LiNTf_2$ and β-CD.

ESI/MS spectra

The ESI/MS spectra of $LiNTf_2$@β-CD (30 mM@30 mM) solution are shown in Fig. 6. Unlike the $LiNTf_2$@β-CD system in diluted solution [39], here we can find not only the 1:1 (NTf_2^--β-CD) complex, but also weak signals of ($2NTf_2^-$-β-CD) and (NTf_2^--2β-CD) complexes. The source of the 1:2 and 2:1 complexes will be explained in the "Discussion" section.

FTIR absorption spectra

In the work about the interaction between $C_n$mimNTf_2 and β-CD, we concluded that a charge resonance equilibrium for NTf_2^- (Scheme 1) exists, and the resonance hybrid II forms the inclusion complex with β-CD [39]. Here we also investigate the structure of NTf_2^- in the $LiNTf_2$@β-CD self-assembly by FTIR. As is shown in Fig. 7, the freeze-dried product of $LiNTf_2$@β-CD (30 mM@30 mM) solution exhibits strong characteristic absorption peaks of NTf_2^- resonance hybrid II at 740.5, 1054.9, and 1197.6 cm^{-1}, while the physical mixture of $LiNTf_2$ and β-CD does not [39]. This indicates that a majority of NTf_2^- turns into the resonance hybrid when the self-assembly is formed in the concentrated solution.

Discussion

Secondary assembly mechanism

The inclusion complexation between NTf_2^- and β-CD has been investigated in the diluted solution [39], while their self-assembly behavior in the concentrated has not. There have been some reports that NTf_2^- self-assemble with the supramolecular host molecules. For instance, Yan et al. prepared a metal organic framework polymer [K(18-crown-6)] [NTf_2] [51]. In the polymer, NTf_2^- coordinated to K^+ with the O-atoms to construct the polymer chains [51]. We are also interested in the supramolecular self-assembly behavior of NTf_2^- and crystallized a new complex of NTf_2^- with Cs^+ and the calixcrown bis(2-propyloxy)-calix [4] crown-6 (BPC6) [52]. The NTf_2^- anion compensates the positive charge of $[Cs\text{-}BPC6]^+$ moiety, and one oxygen atom of a SO_2 group further coordinates with Cs^+. Besides, we have also crystallized Rb^+ and Cs^+ complexes with NTf_2^- and dicyclohexyl-18-crown-6 [53]. In these examples, the coordination interaction between metal ions, NTf_2^-, and host molecules contributes to the formation of the complexes. As for the $LiNTf_2$@β-CD system, no coordination interaction exist, while the hydrogen-bonding plays a more important role, so the self-assembly mode may be different.

In the diluted aqueous solution, NTf_2^- was found to forms the 1:1 inclusion complex with β-CD [39], while in the concentrated $LiNTf_2$@β-CD solutions, the results of DLS and TEM demonstrated the formation of nanosheet structures with regular shape. Before the discussion of self-assembly mechanism, the results of DLS, TEM, and XRD show that the excess $LiNTf_2$ destroys the self-assembly and the excess β-CD form self-aggregates on its own. Besides, the composition of the self-assemblies generated from the $LiNTf_2$@β-CD (150 mM@150 mM) system were demonstrated by elemental analysis to be $LiNTf_2$·1.06β-CD, so we confirmed a 1:1 molar ratio of $LiNTf_2$ to β-CD in the self-assembly.

The XRD results indicate the channel-type arrangement of the β-CD molecules, so in the self-assembly, the inclusion complexes form the nanotube structures. Besides, the FTIR results show that NTf_2^- turns into the resonance hybrid in the self-assembly. These results indicate the formation of the nanotubes based on the NTf_2^-(II)-β-CD inclusion complexes. In addition, the weak signals of ($2NTf_2^-$-β-CD) and (NTf_2^--2β-CD) in ESI/MS spectra, which cannot be detected in the spectra of the diluted $LiNTf_2$ and β-CD solution [39], should originate from the fragments of the nanotubes and the nanosheet. And one NTf_2^- (or β-CD) interacts with two β-CD (or NTf_2^-). We may propose a nanotube structure, which is a common pattern in the CD-based self-assembly. In the nanotube, β-CD molecules are bound together in a channel-type way by the resonance hybrid of NTf_2^- in the CD cavities. And the bridging interaction between the NTf_2^-(II) and two β-CD plays an important role when the NTf_2^-(II)-β-CD inclusion complexes self-assemble into nanotubes.

The regularly shaped nanosheets indicates regular stacking of the nanotubes, so a possible self-assembly mechanism (Scheme 1) is suggested accordingly. In the first stage, NTf_2^- forms individual NTf_2^-@β-CD complexes with β-CD, which self-assemble into one dimensional nanotubes. Afterwards, many of the nanotubes further stack with each other to form 3D sheets by SA.

Taking into consideration of the 1:1 molar ratio of $LiNTf_2$ to β-CD in the self-assembly, we suggest that all the β-CDs cavities in the self-assembly are all occupied by NTf_2^-. This mechanism is similar to the mechanisms in some of the literatures [26–29, 35, 36], but partly different from our previous SA systems [23–25]. In our SA induced

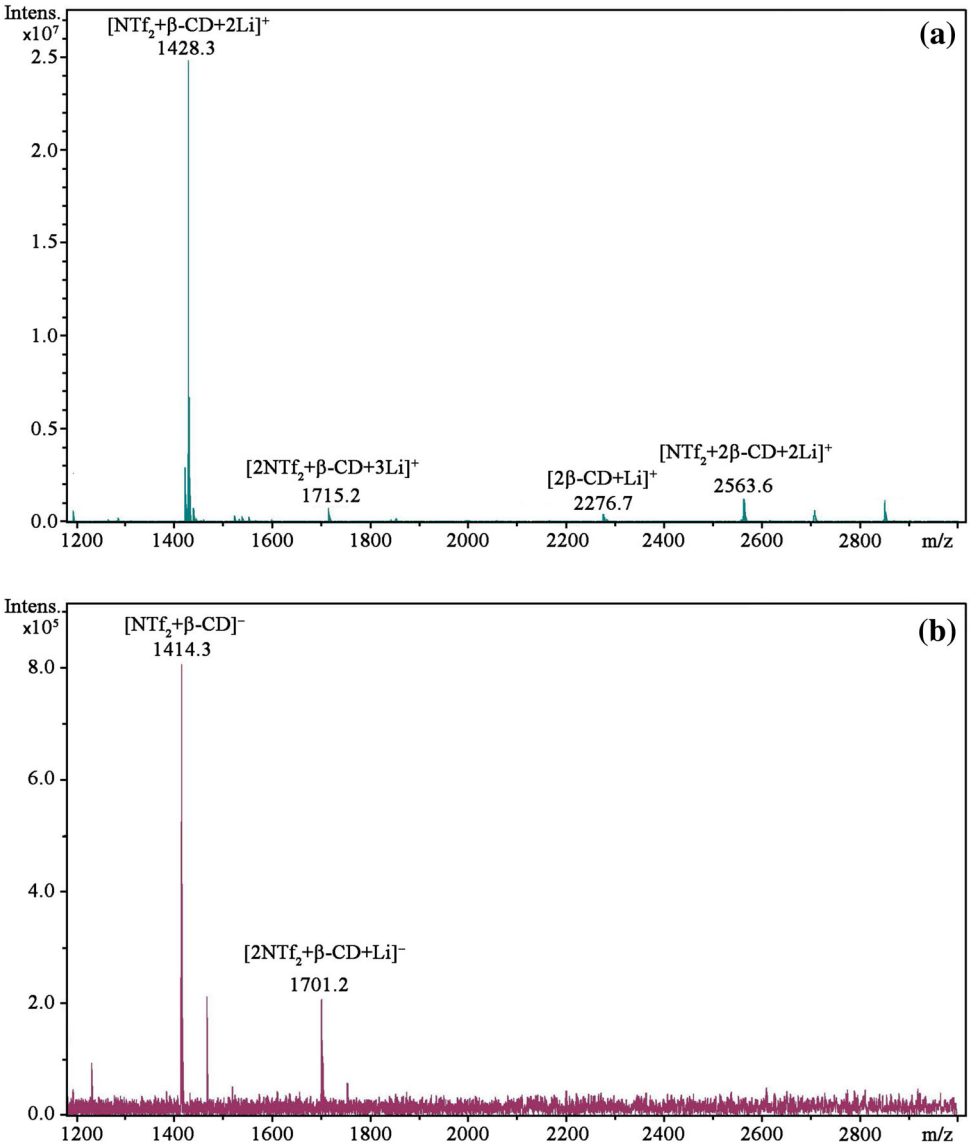

Fig. 6 **a** Positive and **b** negative ESI/MS spectra of the $LiNTf_2$@β-CD (30 mM@30 mM) solution

by organic molecules with poor solubility, the organic molecules first induce β-CDs to form rigid nanotubes, and with these nanotubes as recrystallization centers, other empty β-CDs are packed together to form the rodlike structures [23–25]. Here most β-CDs tend to form inclusion complexes with NTf_2^-, so the SA can be well-organized through the stacking of the NTf_2^--β-CD nanotubes. The concentration of the guest molecule leads to the difference of the SA mechanism between the $LiNTf_2$@β-CD SA system and our previous ones.

Driving forces for self-assembly

The addition of urea influences the self-assembly by weakening the inclusion complexation between NTf_2^- and β-CD, suggesting that hydrophobic interaction is an essential driving force for the self-assembly between $LiNTf_2$ and β-CD. Besides, we replaced β-CD with α-CD, γ-CD, and DM-β-CD for further investigation on the mechanism. The DLS results show that $LiNTf_2$ can self-assemble with β-CD and γ-CD, but not with α-CD. In Park's dye-γ-CD hydrogel system, gelation occurred only in the complex with γ-CD but was absent with α-CD and β-CD [36]. We consider that a cavity with proper size is also important for the binding of the CD into nanotubes, thus no self-assembly occurs in the $LiNTf_2$@α-CD system. As for DM-β-CD, a large part of the hydroxyl groups are replaced by methyl, so the hydrogen-bonding interaction is weakened. The hydrogen-bonding interaction probably contributes to both the binding of β-CD into nanotubes and the SA of the nanotubes into nanosheets, just like our previous studies about the SA [23–25].

Scheme 1 Mechanism of the formation of the $LiNTf_2$@β-CD self-assembly

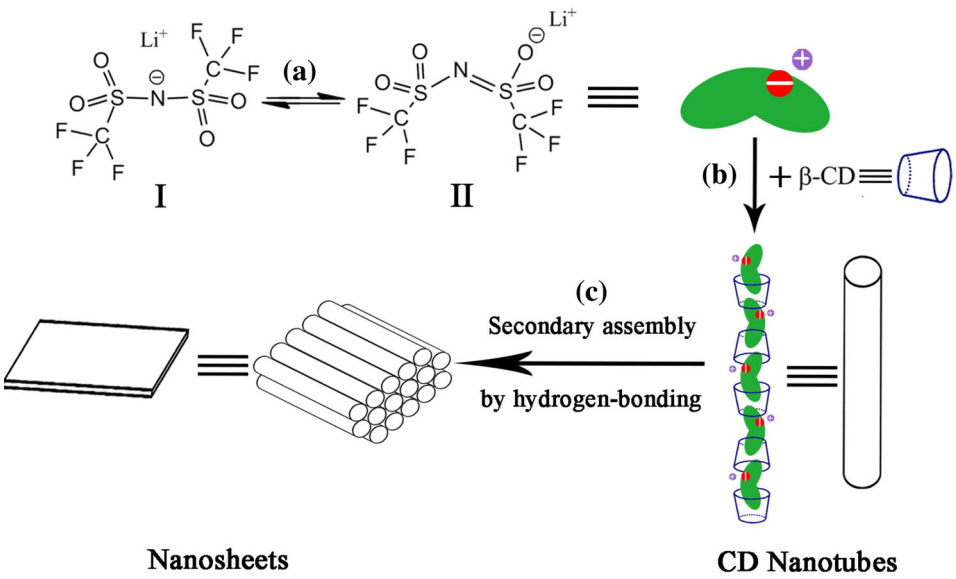

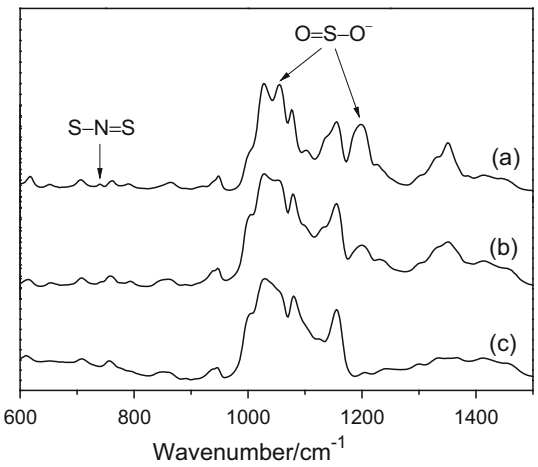

Fig. 7 FTIR absorption spectra of *a* the freeze-dried products of $LiNTf_2$@β-CD (30 mM@30 mM), *b* physical mixture of $LiNTf_2$ and β-CD, and *c* β-CD

In the self-assembly, the arrangement of the nanotubes is perfectly achieved and nanosheets with regular shape are obtained consequently. The thickness of the nanosheets is about 30–40 nm, so it should be noted that the nanosheet is not a single layer but a bulk aggregation of nanotubes. In comparison, Rajendiran et al. also fabricated nanosheets using a series of non-ionic drug molecules and CDs [30–32]. They also proposed the "secondary self-assembly" mechanism [32] while the shape of their nanosheets was irregular. Here the DLS results of the $HNTf_2$, $NaNTf_2$, and $KNTf_2$ systems demonstrate that the undissociated NTf_2^- is unfavorable for self-assembly, and Na^+ and K^+ cannot act the same role as Li^+ in the self-assembly. We attribute these results to the special ability of Li^+ in forming hydrogen-bonding interactions between CDs and water molecules [36, 54–56]. Here Li^+ not only acts as the cation but also makes sure to closely pack the nanotubes into the SA by participating in inducing hydrogen-bonding network between the adjacent β-CDs and water molecules [36, 54–56].

Conclusions

The self-assembly behavior of $LiNTf_2$ and β-CD in the concentrated aqueous solution was investigated on the basis of our previous study about their interaction pattern in the diluted solution. Nanosheets with regular shape were obtained in the $LiNTf_2$@β-CD system. We confirmed that $LiNTf_2$ self-assembles with β-CD in a 1:1 molar ratio. A supramolescular self-assembly mechanism was proposed, that $LiNTf_2$@β-CD firstly forms one dimensional nanotubes, after which the nanotubes further stack with each other to form 3D nanosheets by SA. It was demonstrated that the hydrogen-bonding interaction between adjacent β-CDs molecules is necessary for the formation of the nanotubes and the SA, and Li^+ shows a special effect in the SA by inducing stable hydrogen-bonding network between the adjacent β-CDs and water molecules. By this work we further illustrated our SA mechanism in the concentrated aqueous solution, and obtained a novel self-assembly structure by the SA mechanism. This SA system is helpful in constructing CD self-assembly structures based on inclusion complexation in water. Besides, as NTf_2^- is an important anion of ILs, this work may bring in a new way for the application of IL-CD system, such as synthesis, catalysis, separation, reaction medium, etc.

Acknowledgments This work was financially supported by National Natural Science Foundation of China (Grant No. 91226112 and 21471008).

References

1. He, Y.F., Fu, P., Shen, X.H., Gao, H.C.: Cyclodextrin-based aggregates and characterization by microscopy. Micron **39**, 495–516 (2008)
2. Agbaria, R.A., Gill, D.: Extended 2,5-diphenyloxazole-γ-cyclodextrin aggregates emitting 2,5-diphenyloxazole excimer fluorescence. J. Phys. Chem. **92**, 1052–1055 (1988)
3. Li, G., McGown, L.B.: Molecular nanotube aggregates of β-cyclodextrins and γ-cyclodextrins linked by diphenylhexatrienes. Science **264**, 249–251 (1994)
4. Pistolis, G., Malliaris, A.: Nanotube formation between cyclodextrins and 1,6-diphenyl-1,3,5-hexatriene. J. Phys. Chem. **100**, 15562–15568 (1996)
5. Pistolis, G., Malliaris, A.: Size effect of α, ω-diphenylpolyenes on the formation of nanotubes with γ-cyclodextrin. J. Phys. Chem. B **102**, 1095–1101 (1998)
6. Liu, Y., You, C.C., Zhang, H.Y., Kang, S.Z., Zhu, C.F., Wang, C.: Bis(molecular tube)s: supramolecular assembly of complexes of organoselenium-bridged β-cyclodextrins with platinum(IV). Nano Lett. **1**, 613–616 (2001)
7. Liu, Y., Zhao, Y.L., Zhang, H.Y., Song, H.B.: Polymeric rotaxane constructed from the inclusion complex of β-cyclodextrin and 4,4′-dipyridine by coordination with nickel(II) ions. Angew. Chem. Int. Ed. **42**, 3260–3263 (2003)
8. Liu, Y., Zhao, Y.L., Chen, Y., Guo, D.S.: Assembly behavior of inclusion complexes of β-cyclodextrin with 4-hydroxyazobenzene and 4-aminoazobenzene. Org. Biomol. Chem. **3**, 584–591 (2005)
9. Fan, X.T., Wang, L., Luo, Q., Zhao, L.L., Xu, J.Y., Liu, J.Q., Zheng, Q.C.: Construction of Giant branched nanotubes from cyclodextrin-based supramolecular amphiphiles. Chem. Commun. **51**, 6512–6514 (2015)
10. Hernandez-Pascacio, J., Garza, C., Banquy, X., Diaz-Vergara, N., Amigo, A., Ramos, S., Castillo, R., Costas, M., Pineiro, A.: Cyclodextrin-based self-assembled nanotubes at the water/air interface. J. Phys. Chem. B **111**, 12625–12630 (2007)
11. Mandal, A.K., Das, D.K., Sen Mojumdar, S., Bhattacharyya, K., Das, A.K.: Study of γ-cyclodextrin host-guest complex and nanotube aggregate by fluorescence correlation spectroscopy. J. Phys. Chem. B **115**, 10456–10461 (2011)
12. Agbaria, R.A., Gill, D.: Noncovalent polymers of oxadiazole derivatives induced by γ-cyclodextrin in aqueous-solutions—fluorescence study. J. Photochem. Photobiol. A Chem. **78**, 161–167 (1994)
13. Ohira, A., Sakata, M., Taniguchi, I., Hirayama, C., Kunitake, M.: Comparison of nanotube structures constructed from α-, β-, and γ-cyclodextrins by potential-controlled adsorption. J. Am. Chem. Soc. **125**, 5057–5065 (2003)
14. Wen, X.H., Guo, M., Liu, Z.Y., Tan, F.: Nanotube formation in solution between β-cyclodextrin and cinchonine. Chem. Lett. **33**, 894–895 (2004)
15. El-Kemary, M., Organero, J.A., Santos, L., Douhal, A.: Effect of cyclodextrin nanocavity confinement on the photorelaxation of the cardiotonic drug milrinone. J. Phys. Chem. B **110**, 14128–14134 (2006)
16. Park, C., Im, M.S., Lee, S., Lim, J., Kim, C.: Tunable fluorescent dendron-cyclodextrin nanotubes for hybridization with metal nanoparticles and their biosensory function. Angew. Chem. Int. Ed. **47**, 9922–9926 (2008)
17. Roy, D., Mondal, S.K., Sahu, K., Ghosh, S., Sen, P., Bhattacharyya, K.: Temperature dependence of anisotropy decay and solvation dynamics of coumarin 153 in γ-cyclodextrin aggregates. J. Phys. Chem. A **109**, 7359–7364 (2005)
18. Zhang, C.F., Shen, X.H., Gao, H.C.: Studies on the nanotubes formed by 2-phenyl-5-(4-diphenylyl)1,3,4-oxadiazole and cyclodextrins. Chem. Phys. Lett. **363**, 515–522 (2002)
19. Zhang, C.F., Shen, X.H., Gao, H.C.: Studies on the formation of cyclodextrin nanotube by fluorescence and anisotropy measurements. Spectrosc. Spectr. Anal. **23**, 217–220 (2003)
20. Wu, A.H., Shen, X.H., Gao, H.C.: Cyclodextrin nanotube induced by 4,4′-bis(2-benzoxazolyl) stilbene. Int. J. Nanosci. **5**, 213–218 (2006)
21. Cheng, X.L., Wu, A.H., Shen, X.H., He, Y.K.: The formation of cyclodextrin nanotube induced by POPOP molecule. Acta Phys. Chim. Sin. **22**, 1466–1472 (2006)
22. Wu, A.H., Shen, X.H., He, Y.K.: Investigation on γ-cyclodextrin nanotube induced by N,N'-diphenylbenzidine molecule. J. Colloid Interface Sci. **297**, 525–533 (2006)
23. Wu, A.H., Shen, X.H., He, Y.K.: Micrometer-sized rodlike structure formed by the secondary assembly of cyclodextrin nanotube. J. Colloid Interface Sci. **302**, 87–94 (2006)
24. Zhang, J.J., Shen, X.H., Wu, A.H., Zhang, C.F., Chen, Q.D., Gao, H.C.: Formation of nanotubes and secondary assemblies of cyclodextrins induced by BBOT. Sci. China Chem. **53**, 2019–2025 (2010)
25. He, Y.F., Shen, X.H., Chen, Q.D., Gao, H.C.: Characterization and mechanism study of micrometer-sized secondary assembly of β-cyclodextrin. Phys. Chem. Chem. Phys. **13**, 447–452 (2011)
26. Jaffer, S.S., Saha, S.K., Eranna, G., Sharma, A.K., Purkayastha, P.: Intramolecular charge transfer probe induced formation of α-cyclodextrin nanotubular suprastructures: a concentration dependent process. J. Phys. Chem. C **112**, 11199–11204 (2008)
27. Jaffer, S.S., Saha, S.K., Purkayastha, P.: Fragmentation of molecule-induced γ-cyclodextrin nanotubular suprastructures due to drug dosage. J. Colloid Interface Sci. **337**, 294–299 (2009)
28. Sowmiya, M., Purkayastha, P., Tiwari, A.K., Jaffer, S.S., Saha, S.K.: Characterization of guest molecule concentration dependent nanotubes of β-cyclodextrin and their secondary assembly: study with trans-2-[4(dimethylamino)styryl]benzothiazole, a TICT-fluorescence probe. J. Photochem. Photobiol. A Chem. **205**, 186–196 (2009)
29. Sowmiya, M., Tiwari, A.K., Saha, Eranna, G., Sharma, A.K., Saha, S.K.: Study of the binding interactions of a hemicyanine dye with nanotubes of β-cyclodextrin and effect of a hofmeister series of potassium salts. J. Phys. Chem. C **118**, 2735–2748 (2014)
30. Rajendiran, N., Venkatesh, G., Mohandass, T.: Fabrication of 2D nanosheet through self assembly behavior of sulfamethoxypyridazine inclusion complexes with α- and β-cyclodextrins. Spectrochim. Acta Part A Mol. Biomol. Spectrosc. **123**, 158–166 (2014)
31. Rajendiran, N., Venkatesh, G., Saravanan, J.: Supramolecular aggregates formed by sulfadiazine and sulfisomidine inclusion complexes with α- and β-cyclodextrins. Spectrochim. Acta Part A Mol. Biomol. Spectrosc. **129**, 157–162 (2014)
32. Rajendiran, N., Venkatesh, G.: Micrometer size rod formed by secondary self assembly of omeprazole with α- and β-cyclodextrins. Spectrochim. Acta Part A Mol. Biomol. Spectrosc. **137**, 832–840 (2015)
33. Das, P., Mallick, A., Sarkar, D., Chattopadhyay, N.: Probe-induced self-aggregation of γ-cyclodextrin: formation of extended nanotubular suprastructure. J. Phys. Chem. B **112**, 9600–9603 (2008)
34. Kurkov, S.V., Loftsson, T.: Cyclodextrins. Int. J. Pharm. **453**, 167–180 (2013)

35. Park, J.S., Jeong, S., Ahn, B., Kim, M., Oh, W., Kim, J.: Selective response of cyclodextrin-dye hydrogel to metal ions. J. Incl. Phenom. Macrocycl. Chem. **71**, 79–86 (2011)
36. Park, J.S., Jeong, S., Chang, D.W., Kim, J.P., Kim, K., Park, E.K., Song, K.W.: Lithium-induced supramolecular hydrogel. Chem. Commun. **47**, 4736–4738 (2011)
37. Zhang, J.J., Shen, X.H.: Multiple equilibria interaction pattern between the ionic liquids CnmimPF6 and β-cyclodextrin in aqueous solutions. J. Phys. Chem. B **115**, 11852–11861 (2011)
38. He, Y.F., Chen, Q.D., Xu, C., Zhang, J.J., Shen, X.H.: Interaction between ionic liquids and β-cyclodextrin: a discussion of association pattern. J. Phys. Chem. B **113**, 231–238 (2009)
39. Zhang, J.J., Shi, J.F., Shen, X.H.: Further understanding of the multiple equilibria interaction pattern between ionic liquid and β-cyclodextrin. J. Incl. Phenom. Macrocycl. Chem. **79**, 319–327 (2014)
40. He, Y.F., Shen, X.H.: Interaction between β-cyclodextrin and ionic liquids in aqueous solutions investigated by a competitive method using a substituted 3H-indole probe. J. Photochem. Photobiol. A -Chem. **197**, 253–259 (2008)
41. Zhang, J.J., Shen, X.H.: Temperature-induced reversible transition between vesicle and supramolecular hydrogel in the aqueous ionic liquid-β-cyclodextrin system. J. Phys. Chem. B **117**, 1451–1457 (2013)
42. Shi, J.F., Shen, X.H.: Construction of supramolecular self-assemblies based on the biamphiphilic ionic liquid-β-cyclodextrin system. J. Phys. Chem. B **118**, 1685–1695 (2014)
43. Bonini, M., Rossi, S., Karlsson, G., Almgren, M., Lo Nostro, P., Baglioni, P.: Self-assembly of β-cyclodextrin in water. part 1: Cryo-TEM and dynamic and static light scattering. Langmuir **22**, 1478–1484 (2006)
44. Vij, A., Kirchmeier, R.L., Shreeve, J.M., Verma, R.D.: Some fluorine-containing nitrogen acids and their derivatives. Coord. Chem. Rev. **158**, 413–432 (1997)
45. Li, S., Purdy, W.C.: Cyclodextrins and their applications in analytical-chemistry. Chem. Rev. **92**, 1457–1470 (1992)
46. Shen, X.H., Belletete, M., Durocher, G.: Quantitative study of the hydrophobic interaction mechanism between urea and molecular probes used in sensing some microheterogeneous media. J. Phys. Chem. B **101**, 8212–8220 (1997)
47. Shen, X.H., Belletete, M., Durocher, G.: Studies of the inclusion complexation between a 3H-indole and β-cyclodextrin in the presence of urea, sodium dodecyl sulfate, and 1-propanol. Langmuir **13**, 5830–5836 (1997)
48. Okumura, H., Kawaguchi, Y., Harada, A.: Preparation and characterization of inclusion complexes of poly(dimethylsiloxane)s with cyclodextrins. Macromolecules **34**, 6338–6343 (2001)
49. Jiao, H., Goh, S.H., Valiyaveettil, S.: Inclusion complexes of poly(4-vinylpyridine)-dodecylbenezenesulfonic acid complex and cyclodextrins. Macromolecules **35**, 3997–4002 (2002)
50. Jiang, L.X., Peng, Y., Yan, Y., Huang, J.B.: Aqueous self-assembly of SDS@2β-CD complexes: lamellae and vesicles. Soft Matter **7**, 1726–1731 (2011)
51. Yan, N., Fei, Z.F., Scopelliti, R., Laurenczy, G., Kou, Y., Dyson, P.J.: Crystallisation of inorganic salts containing 18-crown-6 from ionic liquids. Inorg. Chim. Acta **363**, 504–508 (2010)
52. Sun, T.X., Wang, Z.M., Shen, X.H.: Crystallization of cesium complex containing bis(2-propyloxy)calix[4]crown-6 and bis(trifluoromethyl)sulfonyl imide. Inorg. Chim. Acta **390**, 8–11 (2012)
53. Sun, T.X.: Studies on the extraction of Sr, Cs, U, Tc by ionic liquid based systems. Peking University (2013)
54. Li, Z.L., Hao, A.Y., Li, X.: β-Cyclodextrin supramolecular organogels induced by different carboxylic acids that exhibit diverse morphologies. J. Mol. Liq. **196**, 52–60 (2014)
55. Kong, L., Sun, T., Xin, F.F., Zhao, W.J., Zhang, H.C., Li, Z.L., Li, Y.M., Hou, Y.H., Li, S.Y., Hao, A.Y.: Lithium chloride-induced organogel transformed from precipitate based on cyclodextrin complexes. Colloid Surf. A Physicochem. Eng. Asp. **392**, 156–162 (2011)
56. Guo, X.Q., Song, L.X., Du, F.Y., Dang, Z., Wang, M.: Important effects of lithium carbonate on stoichiometry and property of the inclusion complexes of polypropylene glycol and β-cyclodextrin. J. Phys. Chem. B **115**, 1139–1144 (2011)